

Full Aperture Reconstruction of the Acoustic Far-Field Pattern from Few Measurements

Hélène Barucq¹, Chokri Bekkey² and Rabia Djellouli^{3,*}

¹ INRIA Bordeaux Sud-Ouest Research Center, Team Project Magique-3D, & LMA/CNRS UMR 5142, Université de Pau et des Pays de l'Adour, France.

² Faculté des Sciences de Monastir, Tunisia.

³ Department of Mathematics, California State University Northridge & Interdisciplinary Research Institute for the Sciences, IRIS, USA.

Received 28 December 2009; Accepted (in revised version) 15 June 2010

Available online 24 October 2011

Abstract. We propose a numerical procedure to extend to full aperture the acoustic far-field pattern (FFP) when measured in only few observation angles. The reconstruction procedure is a multi-step technique that combines a *total variation* regularized iterative method with the standard Tikhonov regularized pseudo-inversion. The proposed approach distinguishes itself from existing solution methodologies by using an exact representation of the total variation which is crucial for the stability and robustness of Newton algorithms. We present numerical results in the case of two-dimensional acoustic scattering problems to illustrate the potential of the proposed procedure for reconstructing the full aperture of the FFP from very few noisy data such as *backscattering* synthetic measurements.

AMS subject classifications: 35J05, 78A46, 74J20, 65F22, 65T40, 35N05

Key words: Acoustic scattering problem, limited aperture, inverse obstacle problem, ill-posed problem, total variation, Tikhonov regularization, Newton method.

1 Introduction

The determination of the shape of an obstacle from the knowledge of some scattered far-field patterns (FFP), and assuming some a priori knowledge about the characteristics of the surface of the obstacle is one of the most basic problems arising in the inverse scattering field. However, this inverse obstacle problem (IOP) is very difficult to solve from both mathematical and numerical view points due to its ill-posed nature and — to some extent — to its nonlinearity. The numerical determination of the obstacle becomes more

*Corresponding author. *Email addresses:* helene.barucq@univ-pau.fr (H. Barucq), chokri.bekkey@ipeit.rnu.tn (C. Bekkey), rabia.djellouli@csun.edu (R. Djellouli)

challenging when the FFP is not measured entirely around the obstacle but only in a limited sector (limited aperture), which is the case in most applications. Nevertheless, and because of its importance to many applications such as sonar, radar, geophysical exploration, medical imaging and nondestructive testing [1], applied mathematicians and engineers devoted an important effort and attention, in the last three decades, to the design of solution methodologies for solving numerically IOP problems (see for example the overview in [4] and references therein). The numerical results reported in the literature indicate that the success in the reconstruction of the sought-after shape of an obstacle depends strongly on the *quality* of the given FFP measurements: the aperture (range of observation angles) and the level of noise in the data (accuracy of measurements). In particular, there is no hope — at least by the current numerical methods — to solve the IOP when the FFP is measured in small apertures (less than $\pi/4$) even if the data are noise free (see for example [5–8, 10] among others). Consequently, the development of numerical procedures to enrich (increase the size) the set of FFP measurements when given in a small aperture could become a key step for solving efficiently IOP problems. Note that, from a mathematical point of view, it is always possible to extend the FFP *uniquely* to the entire circle S when given in a (continuous) subset of S . This unique determination is due to the analyticity of the FFP [2]. However, the numerical extension from the knowledge of a (discrete) subset of the FFP is a very challenging problem. Indeed, such extension can be formulated as an inverse problem that is *extremely* ill-posed due to the analyticity of the FFP. Therefore, any numerical procedure for extending (enriching) the FFP measurements must address efficiently the ill-posed nature of this inverse problem.

Previous attempts to solve the inverse problem characterizing the extension of the FFP were based on standard L^2 -Tikhonov regularization techniques on the FFP field [9] as well on its first and second derivative [10]. The extension was (to some extent) successful *only* when the range of measurements is given in an aperture larger than $\pi/2$. These procedures fail to address situations of practical interest, that is when only one measurement (backscattering) or very few measurements are available. Recently, the authors suggested a multistep computational procedure that extends few measurements, such as backscattering data, to *full* aperture (360° -aperture) [11]. The proposed procedure employs, in its first two steps, a regularized Newton-type algorithm where the *total variation* (TV) of the FFP is incorporated to restore the stability to the inverse problem. The total variation of the FFP, which can be viewed as the L^1 -norm of the first derivative of the FFP, is evaluated at each Newton iteration approximatively using a finite difference scheme (see Section 3.2 and the appendix in [11]). The first two-steps of the procedure allow to extend the FFP to at least a $\pi/2$ -aperture. The third step of the proposed procedure uses a Tikhonov-type regularization technique that is known to be efficient when the data are given on an aperture larger than $\pi/2$. The results delivered by this procedure are very promising, especially in the presence of low levels of noise in the data. We propose in this paper to modify this reconstruction strategy by employing an *exact* representation of the total variation of the FFP. The use of such an expression is expected to retain more stability and robustness that are needed for the convergence of the Newton algorithm

applied in the first two-steps of the procedure, which in turn will lead to numerical FFP extensions that are less sensitive to the noise level in the original data. The numerical results obtained with this *modified* procedure illustrate its superiority over the procedure suggested in [11], when the original measurements are contaminated with relatively high levels of noise.

2 Problem statement

Let u_∞ be the far-field pattern (FFP) corresponding to the solution u of the direct acoustic scattering problem by an obstacle Ω [2]. Then, u_∞ is an analytical function defined on the unit circle S [2]. Consequently, we can express it as a Fourier series as follows:

$$u_\infty(\theta) = \sum_{n=-\infty}^{\infty} (-i)^n c_n e^{in\theta}, \quad \theta \in S, \tag{2.1}$$

where the complex constants c_n are the Fourier coefficients. The determination of these constants allows to measure the FFP u_∞ on the entire unit circle S .

The computation of the Fourier coefficients c_n when the FFP u_∞ is given at some (few) observation points allows to determine the FFP u_∞ on the entire unit circle S . This extension can be formulated as the following *inverse* Fourier coefficients problem (IFP): *Given a set of M far-field pattern measurements $\tilde{\mathbf{u}}_\infty = [\tilde{u}_\infty(\hat{\theta}_1), \dots, \tilde{u}_\infty(\hat{\theta}_M)]^T$ for one incident plane wave, find the Fourier coefficients vector $\hat{\mathbf{c}} = [\hat{c}_{-N}, \dots, \hat{c}_N]^T$ such that:*

$$\hat{\mathbf{c}} = \arg \min_{\mathbf{c} \in \mathbb{C}^{2N+1}} \|\mathbf{A}\mathbf{c} - \tilde{\mathbf{u}}_\infty\|_2, \tag{2.2}$$

where *argmin* is used to denote that $\hat{\mathbf{c}}$ is the minimizer of the cost function $\|\mathbf{A}\mathbf{c} - \tilde{\mathbf{u}}_\infty\|_2$ over \mathbb{C}^{2N+1} with N being the truncating order of the Fourier series given by Eq. (2.1). A is a $M \times (2N+1)$ matrix given by:

$$\mathbf{A} = \begin{bmatrix} (-i)^{-N} e^{-iN\hat{\theta}_1} & \dots & 1 & \dots & (-i)^N e^{iN\hat{\theta}_1} \\ (-i)^{-N} e^{-iN\hat{\theta}_2} & \dots & 1 & \dots & (-i)^N e^{iN\hat{\theta}_2} \\ \vdots & \vdots & \vdots & \vdots & \vdots \\ (-i)^{-N} e^{-iN\hat{\theta}_M} & \dots & 1 & \dots & (-i)^N e^{iN\hat{\theta}_M} \end{bmatrix}. \tag{2.3}$$

The IFP problem given by Eq. (2.2) is severely ill-posed. The condition number of the matrix A given by Eq. (2.3) increases exponentially as the number of terms N increases [2]. Consequently, it is very difficult to solve numerically IFP since the accuracy of the solution requires N to be relatively large, depending on the frequency. For this reason, a stabilization technique must be incorporated during the solution of Eq. (2.2).

3 The regularized problem

We propose to use the total variation (TV) of the far-field pattern to restore the stability to the IFP problem [13]. Such a technique has been used widely and successfully in image deblurring applications [14–17]. It consists in replacing the minimization problem (2.2) by the following TV-regularized IFP problem:

$$\hat{\mathbf{c}} = \arg \min_{\mathbf{c} \in \mathbb{C}^{2N+1}} \left\{ \frac{1}{2} \|\mathbf{Ac} - \tilde{\mathbf{u}}_\infty\|_2^2 + \mu \mathcal{J}_{TV}(u_\infty) \right\}, \quad (3.1)$$

where $\mu > 0$ is the regularization parameter and \mathcal{J}_{TV} is a regularization operator representing the total variation of the far-field pattern u_∞ . Observe that Acar et al. in [15] proved that the cost function given by Eq. (3.1) is convex and therefore, the minimization problem is well-posed.

Unlike the method proposed in [11], where $\mathcal{J}_{TV}(u_\infty)$ is evaluated numerically using a finite difference scheme (a central first-order derivative), we propose to use an exact characterization of the derivative of the FFP with respect to its Fourier coefficients. Consequently, the total variation is expressed as follows:

$$\mathcal{J}_{TV}(u_\infty) = \|\mathbf{Ac}\|_1. \quad (3.2)$$

We must point out that the penalty term given by Eq. (3.2) is “slightly” different from the exact total variation of the FFP field. More specifically, $\|\mathbf{Ac}\|_1$ is a TV-type regularization term representing the Fréchet derivative of FFP with respect to the Fourier coefficients \mathbf{c} while the exact TV transformation consists in the derivative with respect to the observation angle θ . At the algebraic level, the difference between the two formulations is that the n^{th} column of the TV formulation is just a multiplication (by $i n$) of the n^{th} column of the matrix resulting from the adopted regularization. Our numerical investigation revealed that the exact formulation improves slightly the accuracy delivered by the approximate formulation proposed in [11] while with the proposed formulation the improvement is more significant, as illustrated by the numerical results reported in Section 5.

Observe that the resulting regularized formulation involves a non-differentiable cost function due to the presence of the 1-norm term $\|\mathbf{Ac}\|_1$. The lack of the regularity is a serious defect in the cost function since it rules out the use of efficient numerical procedures, such as Newton algorithms, that require the evaluation of the Jacobians. Hence, in order to restore regularity to the resulting cost function, we modify the FFP total variation term as suggested in [11]. The resulting minimization problem is given by:

$$\hat{\mathbf{c}} = \arg \min_{\mathbf{c} \in \mathbb{C}^{2N+1}} \left\{ \frac{1}{2} \|\mathbf{Ac} - \tilde{\mathbf{u}}_\infty\|_2^2 + \mu \left\| \left((\mathbf{Ac})^2 + \beta^2 \tilde{\mathbf{e}} \right)^{1/2} \right\|_1 \right\}, \quad (3.3)$$

where $\tilde{\mathbf{e}}$ is a vector in \mathbb{C}^{2N+1} given by $\tilde{\mathbf{e}} = [1, \dots, 1]^T$. The bold face exponents in Eq. (3.3), and for the remaining of this section, are pointwise operations on the absolute values

of the vector components. The positive constant β is the *regularity* parameter. Indeed, the presence of β (β large enough) ensures the differentiability of the L^1 -norm term in the cost function given by Eq. (3.3). The optimal value of the couple (μ, β) is obtained using — at this point of the study — a trial and error strategy since our primary goal is to investigate the feasibility of the proposed method. Note that the use of a finite difference approximation of the total variation of the FFP leads to the presence in the formulation of a third parameter h , representing the step size of the discretization scheme.

We note that a serious shortcoming of standard L^2 -regularization techniques is that they do not allow discontinuous solutions, whereas a TV-computed solution could be discontinuous. Therefore, the proposed TV formulation has the potential to be more robust in the presence of noisy data due to measurement errors and/or roundoff.

Similarly to [11], we propose to apply the Newton method to solve the nonlinear minimization problem given by (3.3) since the corresponding cost function is now differentiable. Consequently, at each Newton iteration \mathbf{m} , we solve the linear system:

$$\mathcal{F}''(\mathbf{c}^{(\mathbf{m})})\delta\mathbf{c}^{(\mathbf{m})} = -\mathcal{F}'(\mathbf{c}^{(\mathbf{m})}) \quad (3.4)$$

and then update

$$\mathbf{c}^{(\mathbf{m}+1)} = \mathbf{c}^{(\mathbf{m})} + \delta\mathbf{c}^{(\mathbf{m})}. \quad (3.5)$$

\mathcal{F}'' is a $(2N+1) \times (2N+1)$ matrix representing the Hessian of the regularized cost function. \mathcal{F}'' is given by:

$$\mathcal{F}''(\mathbf{c}^{(\mathbf{m})}) = \mathbf{A}^* \mathbf{A} + \mu \left(\mathbf{A}^* \Psi^{-1} \mathbf{A} - \mathbf{A}^* \left[\text{diag} \left(\mathbf{A} \mathbf{c}^{(\mathbf{m})} \right) \right]^2 \Psi^{-3} \mathbf{A} \right), \quad (3.6)$$

where Ψ is a $(2N+1) \times (2N+1)$ diagonal matrix given by:

$$\Psi = \text{diag} \left(\left[\left[\mathbf{A} \mathbf{c}^{(\mathbf{m})} \right]^2 + \beta^2 \tilde{\mathbf{e}} \right]^{1/2} \right). \quad (3.7)$$

$\mathcal{F}'(\mathbf{c}^{(\mathbf{m})})$ is a vector in \mathbb{C}^{2N+1} representing the Jacobian of the regularized cost function given by (3.3). $\mathcal{F}'(\mathbf{c}^{(\mathbf{m})})$ is defined by:

$$\mathcal{F}'(\mathbf{c}^{(\mathbf{m})}) = \mathbf{A}^* \left(\mathbf{A} \mathbf{c}^{(\mathbf{m})} - \tilde{\mathbf{u}}_\infty \right) + \mu \mathbf{A}^* \Psi^{-1} \mathbf{A} \mathbf{c}^{(\mathbf{m})}. \quad (3.8)$$

Observe that each Newton iteration equation consists in solving a $(2N+1) \times (2N+1)$ linear system which can be done easily with an LU factorization method since this system is, in practice, *small*. Indeed, $2N+1$ represents the number of modes left in the truncated Fourier series given by Eq. (2.1).

4 The multi-step procedure for the FFP extension

Similarly to [11], we adopt the following three-step procedure for extending the FFP to *full* aperture:

Step 1. The given data in this step are the frequency regime ka (a characterizes the dimension of the scatterer, and k being the wavenumber), the truncation order of the Fourier series (see Eq. (2.1)) N , and the number of FFP measurements M . The value of N depends on ka . Typically, $N \approx ka$, which means $2ka + 1$ modes are left in the truncated series. The FFP data $\tilde{\mathbf{u}}_\infty = [\tilde{u}_\infty(\hat{\theta}_1), \dots, \tilde{u}_\infty(\hat{\theta}_M)]^T$ are measured at M points in a given observation sector, as depicted in Fig. 1. Next, apply a multi-stage strategy to enrich -at each stage- the FFP measurements by only *two* additional adjacent values. More specifically, the proposed strategy requires the following:

Step 1.1. Solve the TV-regularized minimization problem (3.3) using Newton iteration equations (3.4)-(3.5). Proceed as follows:

- Initialize the Fourier coefficient vector $\mathbf{c} = \mathbf{c}^{(0)}$ and compute the FFP $\mathbf{u}_\infty^{(0)}$ corresponding to $\mathbf{c}^{(0)}$.
- For a given μ and β , apply the Newton algorithm to the solution of the regularized IFP problem given by Eq. (3.3) until convergence/stagnation of the residual which is the 2-norm of the relative error on the FFP, i.e.

$$\frac{\left(\sum_{j=1}^M |u_\infty^{(m)}(\hat{\theta}_j) - \tilde{u}_\infty(\hat{\theta}_j)|^2 \right)^{\frac{1}{2}}}{\left(\sum_{j=1}^M |\tilde{u}_\infty(\hat{\theta}_j)|^2 \right)^{\frac{1}{2}}} < \epsilon_1,$$

where $\mathbf{u}_\infty^{(m)}$ is the computed FFP at Newton iteration m and ϵ_1 is a prescribed tolerance. ϵ_1 is typically the noise level in the original data.

- Compute the new FFP and store its values at $M+2$ observation points. These points are the ones located at the original M measurements and 2 additional points that are adjacent to the initial ones, as depicted in Fig. 2(a). Note that the values of the original FFP data are *replaced* by the computed ones. Hence, at the end of this step, the FFP data are enriched by two *new* observation points and the original measurements are *updated* by the computed ones. Also, store the Fourier coefficients vector denoted by $\mathbf{c}^{[1]} = [c_{-N}^{[1]}, \dots, c_0^{[1]}, \dots, c_N^{[1]}]^T$ corresponding to the FFP computed at the last iteration of the Newton algorithm. We must point out that we have performed several numerical experiments with and without updating the FFP

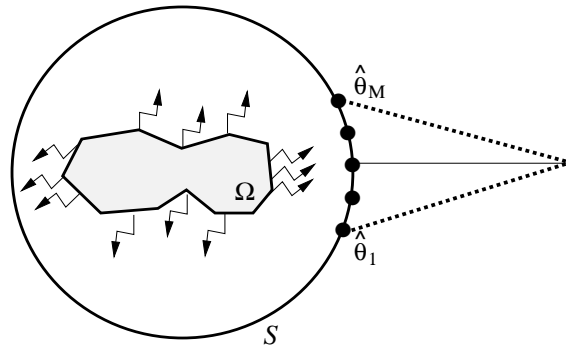
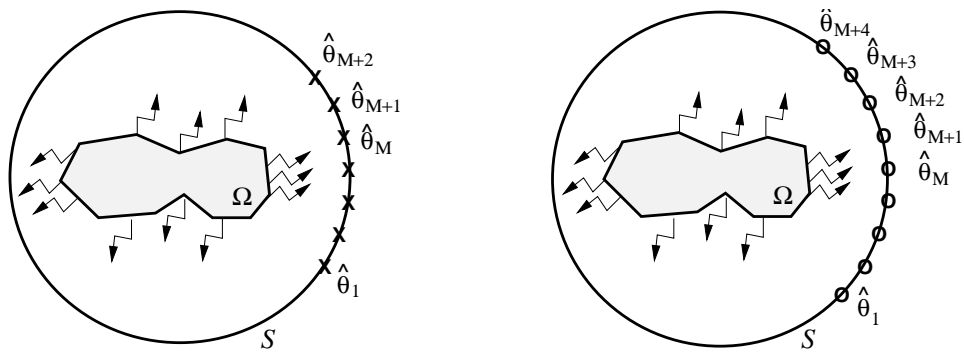


Figure 1: The given (few) FFP measurements for Step 1 are located at points represented by "•".



(a) The Given FFP data are extended at the end of Step 1.1 by 2 measurements located at $\hat{\theta}_1$ and $\hat{\theta}_{M+2}$.

(b) The computed FFP measurements in Fig.2(a) are extended at the end of Step 1.2 by 2 measurements located at $\hat{\theta}_1$ and $\hat{\theta}_{M+4}$.

Figure 2: Extension process of the FFP in Step 1.

measurements. We found that replacing the data by the computed ones leads to better reconstruction of the FFP field.

Step 1.2. Repeat the solution procedure described in Step 1.1 where — this time — the FFP measurements (the reference solution for the Newton algorithm) are the $M+2$ values of the FFP computed and stored in Step 1.1, i.e., $\tilde{\mathbf{u}}_\infty = [\tilde{u}_\infty(\hat{\theta}_1), \dots, \tilde{u}_\infty(\hat{\theta}_M), \tilde{u}_\infty(\hat{\theta}_{M+1}), \tilde{u}_\infty(\hat{\theta}_{M+2})]^T$. Now, the stopping criterion of the Newton algorithm is the 2-norm of the residual at the $M+2$ observation points, that is:

$$\frac{\left(\sum_{j=1}^{M+2} |u_\infty^{(m)}(\hat{\theta}_j) - \tilde{u}_\infty(\hat{\theta}_j)|^2 \right)^{\frac{1}{2}}}{\left(\sum_{j=1}^{M+2} |\tilde{u}_\infty(\hat{\theta}_j)|^2 \right)^{\frac{1}{2}}} < \epsilon_1.$$

Then,

- Compute the new FFP and store its values at $M+4$ observation points. These points are the ones located at the previous $M+2$ measurements plus 2 additional points that are adjacent to the previous ones, as depicted in Fig. 2(b). Hence, the values of the original $M+2$ FFP data are *updated* by the computed ones. Observe that, at the end of this step, the *original* M FFP data are *updated* and *enriched* by four measurements.
- Store the Fourier coefficients vector denoted by $\mathbf{c}^{[2]} = [c_{-N}^{[2]}, \dots, c_0^{[2]}, \dots, c_N^{[2]}]^T$ corresponding to the FFP computed at the last iteration of the Newton algorithm.

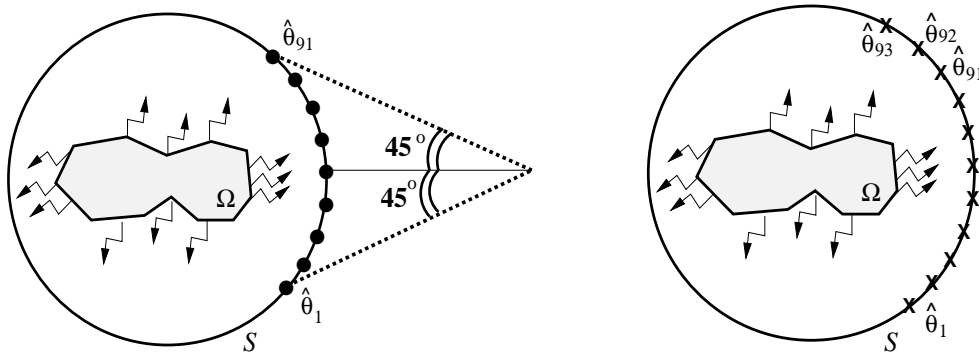
Step 1.3. Repeat this multi-stage process until its stagnation, i.e., the values of the Fourier coefficients vector — stored each time — are no longer changing:

$$\|\mathbf{c}^{[m+1]} - \mathbf{c}^{[m]}\|_2 = \left(\sum_{j=-N}^N |c_{-N}^{[m+1]} - c_{-N}^{[m]}|^2 \right)^{\frac{1}{2}} < \epsilon_2,$$

where ϵ_2 is a fixed tolerance. Typically, $\epsilon_2 \approx 10^{-6}$. At stagnation, compute the new FFP and store its values in an aperture of 90° , that is $\tilde{\mathbf{u}}_\infty = (\tilde{u}_\infty(\hat{\theta}_1), \dots, \tilde{u}_\infty(\hat{\theta}_{91}))$. These values are located in the sector of the original measurements, as depicted in Fig. 3(a).

Step 2. Repeat the multi-stage procedure described in Step 1 using this time the following initial data:

- The number of Fourier coefficients is increased by 2, i.e., $N \leftarrow (N+1)$.



(a) The initial FFP measurements in Step 2 are given in a 90° aperture. These data are obtained at the end of Step 1.

(b) The computed FFP measurements in Fig. 3(a) are extended at the end of Step 2.1 by 2 measurements located at $\hat{\theta}_1$ and $\hat{\theta}_{93}$.

Figure 3: Extension process of the FFP in Step 2.

- The FFP measurements are the values the computed FFP at the end of Step 1.3. These measurements are given in an aperture of 90° i.e. $M \leftarrow 91$ (see Fig. 3(a)).

At stagnation (at the end of Step 2), compute the new FFP and store its values at $91+2P$ new observation points (the number of extended FFP measurements is always *even*). These points are the ones located in the region of the previous 90° aperture measurements plus $2P$ additional points that are adjacent to them. Hence, at the end of step 2, the FFP is computed over an aperture of $(90+2P)^\circ$ (for $P=1$, see Fig. 3(b)).

Step 3. The full aperture of the FFP is computed in this step using a Tikhonov regularized pseudo-inversion. More specifically, starting with FFP values computed and stored at the end of Step 2, i.e. $\tilde{\mathbf{u}}_\infty = [\tilde{u}_\infty(\hat{\theta}_1), \dots, \tilde{u}_\infty(\hat{\theta}_{91+2P})]^T$, proceed as follows:

- First, compute the *final* values of the Fourier coefficients $\hat{\mathbf{c}} = [\hat{c}_{-N-1}, \dots, \hat{c}_0, \dots, \hat{c}_{N+1}]^T$ by solving the linear system:

$$\hat{\mathbf{c}} = (\mathbf{A}^* \mathbf{A} + \mu \mathbf{I})^{-1} \mathbf{A}^* \tilde{\mathbf{u}}_\infty,$$

where μ is the regularization parameter chosen using a trial and error strategy.

- Then, evaluate the *full* aperture of the FFP using the Fourier series expansion:

$$\tilde{u}_\infty(\theta) = \sum_{n=-N-1}^{N+1} (-i)^n \hat{c}_n e^{in\theta}, \quad \theta \in [0, 2\pi).$$

Observe that this three-step methodology requires solving mainly $(2N+1) \times (2N+1)$ linear systems which are *small-scale* systems, since $2N+1$ is the number of Fourier modes in the truncated series. Therefore, these linear system can be easily solved using direct methods such as the standard *LU* factorization. Note that the number of these systems depends however on the number of Newton iterations (typically no more than 10 iterations) and the number of trials — at each Newton iteration — to select the “best” values of the parameters μ and β (about 40 trials).

5 Illustrative numerical results

We have performed several numerical experiments to assess the effect of the noise level on the accuracy of the FFP extension when using the proposed three-step procedure equipped with the exact characterization of the FFP total variation. We have compared the obtained results to the ones delivered by the method when using a finite difference (FD) approximation [11]. Because of space limitations, we present the results obtained when the given data are measured at (a) one observation angle, $M=1$ (for a backscattering measurement) and (b) three backscattering observation angles, $M=2$ (corresponding to

Table 1: Sensitivity of the 2-norm relative error of the full aperture extended FFP field to the white noise level. Case of one backscattering measurement ($M=1$) and $ka=1$.

Noise level	Extension over 360° with	
	exact $\mathcal{J}_{TV}(u_\infty)$	approximate $\mathcal{J}_{TV}(u_\infty)$
1%	13.2157 %	11.9970 %
5%	15.5433 %	21.3259 %
10%	16.3817 %	24.7173 %

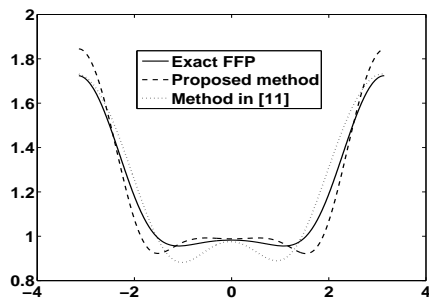
Table 2: Sensitivity of the 2-norm relative error of the full aperture extended FFP field to the noise level. Case of a two-degree backscattering aperture ($M=3$) and $ka=1$.

Noise level	Extension over 360° with	
	exact $\mathcal{J}_{TV}(u_\infty)$	approximate $\mathcal{J}_{TV}(u_\infty)$
1%	11.7352 %	12.5250 %
5%	11.4183 %	11.3946 %
10%	12.8643 %	19.3652 %

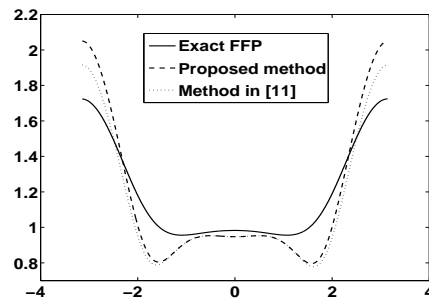
very few measurements). Note that these measurements are synthetic data corresponding to the acoustic scattered field by a *sound-soft* disk-shaped scatterer, that can be computed analytically [2, 18]. In all experiments, we have set $ka=1$ and considered three levels of white noise (in the 2-norm sense): 1% (low), 5% (medium), and 10% (high). The results are reported in Figs. 4-5 and Tables 1-2. The following observations are noteworthy:

- In all cases, the proposed procedure is able to reconstruct the full FFP aperture with an impressive level of accuracy. For example, in the case of high level of white noise (10%), the procedure delivers full aperture with a relative error of about 16% in the case of one backscattering measurement, and of about 13% in the case of three backscattering measurements (see Tables 1-2). Note that such a precision is of a great interest since it has been demonstrated that one can retrieve the shape of the scatterer when the data are tainted with a noise level as high as 20% [10]. Furthermore, applying the denoising procedure suggested in [12] could reduce the level of errors on the reconstructed FFP field, and therefore may improve the accuracy level.

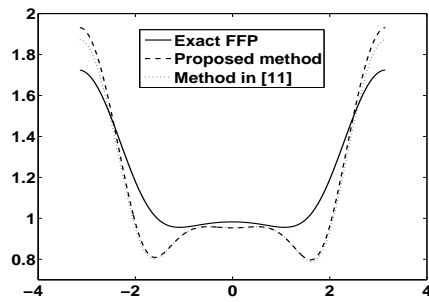
- The results reported in Tables 1-2 clearly indicate that the proposed three-step procedure when equipped with the exact representation of the FFP total variation outperforms the formulation adopted in [11], especially if the original measurements are tainted with a medium or a high noise level. For example, in the presence of a high noise level in the data (10%), the proposed method reduces the relative error on the full FFP reconstructed field from 24.7% to 16.3% in the case of one backscattering measurement, and from 19.3% to 12.8% in the case of three backscattering measurements. In addition, these results tend to indicate that the proposed procedure is less sensitive to the noise than the method proposed in [11]. However, the difference between the two methods is barely noticeable in the presence of a very low noise level (less than 1%).



(a) Noise level: 1%.

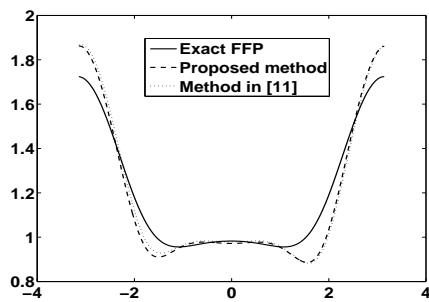


(b) Noise level: 5%.

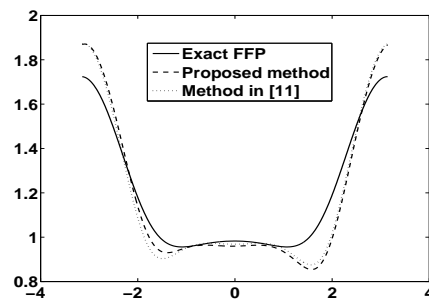


(c) Noise level 10%.

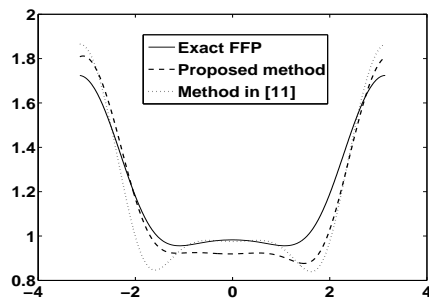
Figure 4: Sensitivity of the reconstruction to the white noise level: Absolute value of the *full* aperture FFP extension from a *one* backscattering measurement ($M = 1$) and $ka = 1$.



(a) Noise level: 1%.



(b) Noise level: 5%.



(c) Noise level: 10%.

Figure 5: Sensitivity of the reconstruction to the noise: Absolute value of the *full* aperture FFP extension from a *two-degree* backscattering measurements ($M = 3$) and $ka = 1$.

- The numerical investigation has revealed that, similarly to the method suggested in [11], Step 1 usually stagnates after reconstructing the FFP field over a 16° -sector, whereas Step 2 stagnates when the FFP field is extended over a 96° -aperture at most. In addition, unlike the method suggested in [11], the proposed procedure is able to reconstruct the full aperture with an acceptable accuracy level using Step 1 only, when the FFP data are measured at one observation angle (one backscattering measurement) with a low noise level (1%), as indicated in Fig. (4) and Table 1.

6 Summary and conclusion

The multi-step procedure proposed in [11] for extending the FFP data has been modified via the use of the exact representation of the FFP total variation. The numerical investigation performed in the case where only one or three backscattering FFP measurements are available revealed that the modified procedure is less sensitive to the noise and clearly outperforms the original method. In particular, the modified extension procedure improves significantly the accuracy level in the full aperture reconstructed FFP field when the FFP data are tainted with a noise level larger than 5%. This impressive success in reconstructing the FFP field over the full aperture from very few and highly noisy measurements has the potential to improve the performance of the existing inverse obstacle solvers in the case of limited aperture. This may be achieved by applying the proposed procedure, as a pre-processing step, to enrich the limited aperture data in order to be used by the considered inverse solver.

Acknowledgments

The authors acknowledge the support by INRIA/CSUN Associate Team Program and by ANR/AHPI research program (Agence Nationale de la Recherche/Analyse Harmonique et Problèmes Inverses). Any opinions, findings, conclusions or recommendations expressed in this material are those of the authors and do not necessarily reflect the views of ANR, CSUN, or INRIA.

References

- [1] C. R. Vogel, *Computational Methods for Inverse Problems*, Frontiers in Applied Mathematics, Society for Industrial and Applied Mathematics (SIAM), Philadelphia, PA, 2002.
- [2] D. Colton and R. Kress, *Inverse Acoustic and Electromagnetic Scattering Theory*, Applied Mathematical Sciences 93, Springer-Verlag, 1992.
- [3] J. Hadamard, *Lectures on Cauchy's Problem in Linear Partial Differential Equations*, Yale University Press, 1923.
- [4] R. Djellouli, *Inverse Acoustic Problems*, In: *Computational Methods for Acoustics Problems*, (F. Magoulès, editor), Saxe-Coburg Publications, (2008), pp. 263–294.

- [5] R. L. Ochs, The limited aperture problem of inverse acoustic scattering: Dirichlet boundary conditions, *SIAM J. Appl. Math.* 47, (1987), pp. 1320–1341.
- [6] A. Zinn, On an optimization method for full- and limited-aperture problem, In: inverse acoustic scattering for a sound-soft obstacle, *Inverse Problems*, 5, (1989), pp. 239–253.
- [7] R. Kress, Integral equations methods in inverse acoustic and electromagnetic scattering, In: *Boundary Integral Formulations for Inverse Analysis*, (Ingham and Wrobel, eds.), Computational Mechanics Publications, Southampton, (1997), pp. 67–92.
- [8] R. Kress, W. Rundell, Inverse obstacle scattering using reduced data, *SIAM J. Appl. Math.*, 59, (1999) pp. 442–454.
- [9] F. Oukaci, Quelques problèmes numériques d'identification de forme en diffraction acoustique, Ph. D. Thesis, Université de Technologie de Compiègne, 1999.
- [10] R. Djellouli, R. Tezaur, and C. Farhat, On the solution of inverse obstacle acoustic scattering problems with a limited aperture, in: *Mathematical and Numerical Aspects of Wave Propagation* (Cohen et al. eds.), Jyväskylä, (2003), pp. 625–630.
- [11] H. Barucq, C. Bekkey, and R. Djellouli, A Multi-Step Procedure for Enriching Limited Two-Dimensional Acoustic Far-Field Pattern Measurements, INRIA Research Report, No. 7048 (2009). Available online at: <http://hal.archives-ouvertes.fr/inria-00420644/fr/>.
- [12] Y. Olshansky, I. Stainvas, and E. Turkel, Simultaneous Scatterer Shape Estimation and Far-Field Pattern Denoising, in: *Proceedings of the ninth International Conference on Mathematical and Numerical Aspects of Wave Propagation* (Barucq et al. eds.), Pau, (2009), pp. 306–307.
- [13] C. R. Vogel, Total Variation regularization for ill-posed problems, Department of Mathematical Sciences Technical Report (1993), Montana State University.
- [14] L. I. Rudin, S. Osher and E. Fatemi, Nonlinear total variation based noise removal algorithms, *Proceeding of the 11th Annual International Conference of the center for Nonlinear Studies, Physica D*, Vol.60 (1992), pp. 259-268.
- [15] R. Acar and C. R. Vogel, Analysis for Bounded Variation Penalty Methods for Ill-Posed Problems, *Inverse Problems*, Vol. 10, No. 6 (1994), pp.1217-1229.
- [16] C. Hansen, Regularization Tools: a Matlab Package for Analysis and Solution of Ill-Posed Problems, *Numerical Algorithms*, 6, (1994), pp. 1-35.
- [17] J. Pedersen, Modular Algorithms for Large-Scale Total Variation Image Deblurring, Master Thesis, Technical University of Denmark, 2005.
- [18] J.J. Bowman, T.B.A. Senior, P.L.E. Uslenghi, *Electromagnetic and Acoustic Scattering by Simple Shapes*, North-Holland Publishing Company, Amsterdam, 1969.